

# Cyclic Fracture Behaviour of Brazed Martensitic Stainless Steel Joints

Hans-Jakob Schindler <sup>2</sup>, Christian Leinenbach <sup>1</sup>, Tanya Baser <sup>1</sup>

<sup>1</sup>*EMPA - Swiss Federal Laboratories for Materials Testing and Research, Dübendorf, Switzerland;* <sup>2</sup>*MatTec AG, Winterthur, Switzerland*

## Abstract

In the present work, the cyclic fracture behaviour of brazed joints of the soft martensitic stainless steel X3CrNiMo13-4 was investigated. The fatigue crack propagation curves ( $da/dN-\Delta K$ ) were derived for different load ratios  $R$ . The fatigue crack threshold values  $\Delta K_{th}$  were estimated to be  $9 \text{ MPa m}^{0.5}$ ,  $7 \text{ MPa m}^{0.5}$  and  $6 \text{ MPa m}^{0.5}$  for the  $R$  values of 0.1, 0.3 and 0.5, respectively. In addition, crack growth curves were derived for different constant loads  $\Delta F$ . The Paris exponent,  $n$ , was found to be very high compared to homogeneous materials and indicating that braze joints have a different cyclic fracture behaviour than bulk materials. The work was completed by SEM investigations of the fractured specimens.

Keywords: Brazing, fatigue crack propagation, crack growth threshold, paris law.

## 1. Introduction

Brazing stainless steel becomes more economical and efficient with the use of advanced furnace brazing methods [1]. High temperature (HT) furnace brazing is a quick and low-cost brazing method to produce strong joints and it is used in the aerospace and other industries as well as for power generation, e.g. compressor impellers or turbine parts [2]. These components are used under complex loading conditions in service, e.g. mechanical, thermal or thermo-mechanical loads [3]. Brazed joints generally have a lower fatigue life than the base metallic materials, which can be related to the thermal expansion stress during brazing. [4]. Under mechanical loading, complex triaxial stresses form in the thin brazing zone due to the different elastic-plastic properties of the filler metal and the base material and the constraining effect of the base material. As a result, the ultimate tensile strength of the bond can be several times higher than the strength of the unconstrained layer material [5]. Defects such as incomplete gap filling, pores or cracks may be formed during brazing and they can act as stress concentration sites in the brazing zone. Under cyclic mechanical loading, fatigue cracks can initiate and propagate from these defects, leading to spontaneous failure [3]. Therefore, defect assesment of brazed components should be considered.

Fatigue fracture assessment is also of great importance providing structural reliability. Understanding the fatigue crack propagation processes in the brazing zone is significant for service life estimations. The fatigue crack growth behaviour of materials is generally characterized by measuring the fatigue crack growth curves ( $da/dN-\Delta K$ ) at a given load ratio  $R$  [6]. The crack growth increment per cycle,  $da/dN$ , can be related to the applied stress intensity range,  $\Delta K$ , via the Paris equation ( $da/dN=C \Delta K^n$ ) where  $C$  and the exponent  $n$  are experimentally measured material constants [3, 4, 6-10]. Due to the above mentioned stress triaxiality, fatigue crack initiation and propagation in brazed components are of a much more complex nature than in bulk materials. Only a few studies on the fatigue behaviour of brazed joints are reported in the literature [3, 4]. Up to now no data were found for fatigue crack propagation in brazed components.

The aim of the present study was to investigate the fracture behaviour of HT brazed specimens of the soft martensitic stainless steel X3CrNiMo13-4 under cyclic loading. The crack propagation behaviour of brazed steel joints was investigated on a microstructural level by SEM on fractured specimens.

## 2. Materials and method

### 2.1. Base material and filler metals

In this study, the soft martensitic stainless steel X3CrNiMo13-4 was used as base material. The chemical composition of the martensitic stainless steel X3CrNiMo13-4 is given in Table 1. As filler metal, foils of the binary alloy Au-18Ni with a thickness of 100  $\mu\text{m}$  were applied.

Table 1. Chemical composition of X3CrNiMo13-4.

Element	C	Si	Mn	P	S	Cr	Mo	N	Ni
Min.						12.00	0.30	0.02	3.50
Max.	0.05	0.70	1.50	0.04	0.01	14.00	0.70		4.50

### 2.2. Brazing, heat treatment and specimen preparation

Cuboidal steel plates with the dimensions 300x100x25 mm were brazed using a special brazing jig. Brazing was performed in an industrial shielding gas furnace (SOLO Profitherm 600) at a temperature of 1020°C for 20 minutes. Hydro-Argon 7 (93 vol.-% Ar, 7 vol.-% H<sub>2</sub>) was used as shielding gas. The addition of hydrogen to the argon allows removing the oxide film on the stainless steel

surface, which is essential for filler metal wetting. After brazing, the specimens were tempered at 520 °C for 5.5 h in nitrogen atmosphere. A homogenous braze joint with a brazing zone width of approximately 150 μm was obtained with this process. The mechanical properties of the base material and of the braze joint are summarized in Table 2 [3].

Table 2. Mechanical properties of X3CrNiMo 13-4 and X3CrNiMo13-4 – Au-18Ni braze joints.

	R <sub>p0.2</sub> [MPa]	R <sub>m</sub> [MPa]	A <sub>5</sub> [%]	□ <sub>e</sub> [MPa]	□ <sub>max</sub> [MPa]	K <sub>IC</sub> [MPa m <sup>0.5</sup> ]
X3CrNi 13-4	920 ± 5	975 ± 25	17.5 ± 2.5	620 ± 5	660 ± 10	270
X3CrNi13-4 - AuNi18	923 ± 7	976 ± 15	6 ± 0.5	245 ± 10	539 ± 7	49±1.5

The cyclic fracture behaviour was investigated using Double Cantilever Beam (DCB) specimens with the dimensions Bx2hxt=90x60x8 mm (Fig 1). For all specimens, the brazing zone was positioned in the middle of the specimens. After machining of the DCB specimens a notch was introduced into the brazing zone by electro discharge machining (EDM) using a wire with a diameter of 0.3 mm. The stress intensity for mode I loading, K<sub>I</sub>, as a function of the specimen geometry and the applied load can be calculated according to

$$K_I = \frac{F}{Bh^{0.5}} \left( 8 + 13.25 \frac{a}{h} + 12 \left( \frac{a}{h} \right)^2 \right)^{0.5} \quad (\text{Eq. 1})$$

where F is the applied force, B and h the specimen geometry as described above, and a the total crack length measured from the load initiation point.

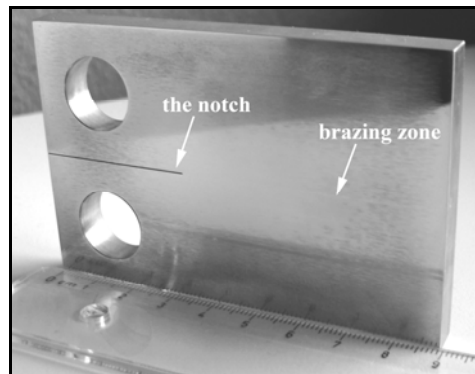


Fig. 1. Geometry of the DCB specimen.

### 2.3. Experimental procedures

Fatigue crack propagation tests were performed on a resonant testing machine (Rumul Type 8601). The load form was sinusoidal constant amplitude. The specimens were cycled at resonant frequencies in the range of 60-65 Hz at different load ratios  $R$  of 0.1, 0.3 and 0.5, respectively. In order to measure the crack length accurately, both side faces of the specimens were carefully polished. The crack length was periodically measured using two travelling light microscopes on both sides of the DCB specimen. The fatigue threshold value  $\Delta K_{th}$  is defined as an asymptotic value of the stress intensity factor range  $\Delta K$  when the propagation rate  $da/dN$  approaches zero [11, 12]. In this study,  $\Delta K_{th}$  was determined according to the ASTM E647 constant  $R$  load reduction test method [13]. In addition, the crack length as a function of the number of loading cycles was measured in constant load amplitude tests at  $R=0.1$ . Fractured specimens were investigated by using a Leica M420 stereo microscope and Philips-FEG XL30 scanning electron microscope (SEM).

## 3. Results

### 3.1. Cyclic fracture behaviour

The fatigue crack growth rates,  $da/dN$ , as a function of the stress intensity range,  $\Delta K$ , are plotted in Fig 2. It should be noted that the difference in the measured crack length on the two side surfaces of the specimens was negligible. Hence, the average crack length was quoted to calculate  $\Delta K$  values. The  $da/dN$ - $\Delta K$  curves have a quite linear shape on the double logarithmic scale. The curves could not be clearly divided into the threshold range, the Paris range and the fast crack propagation range. Rather scattered data were obtained at low crack growth rates. The fatigue crack threshold values,  $\Delta K_{th}$ , which were defined as the stress intensity ranges at which the crack propagation rates  $da/dN$  achieved values of  $10^{-10}$  m/cycle, were estimated to be  $\Delta K_{th} = 9 \text{ MPa}^{0.5}$ ,  $\Delta K_{th} = 7 \text{ MPa}^{0.5}$ ,  $\Delta K_{th} = 6 \text{ MPa}^{0.5}$  corresponding to load ratios of  $R = 0.1$ ,  $R = 0.3$  and  $R = 0.5$ . The  $da/dN$ - $\Delta K$  curves are shifted to lower values of  $\Delta K$ , whereas the slope remains almost constant. A curve fit according to the Paris equation was performed for crack propagation rates between  $10^{-9}$  and  $10^{-5}$  m/cycles. The  $C$  and  $n$  parameters as estimated for the different  $R$  values are listed in Table 3. According to the high slopes of the  $da/dN$ - $\Delta K$  curves, the obtained Paris exponents,  $n$ , are very high compared to homogenous materials [7, 14]. This indicates that fatigue crack growth rate of brazed components is rather sensitive to the applied load range. In addition, it was observed that the Paris exponent increased slightly with an increasing  $R$  value, indicated that crack growth is even more accelerated at higher load ratios.

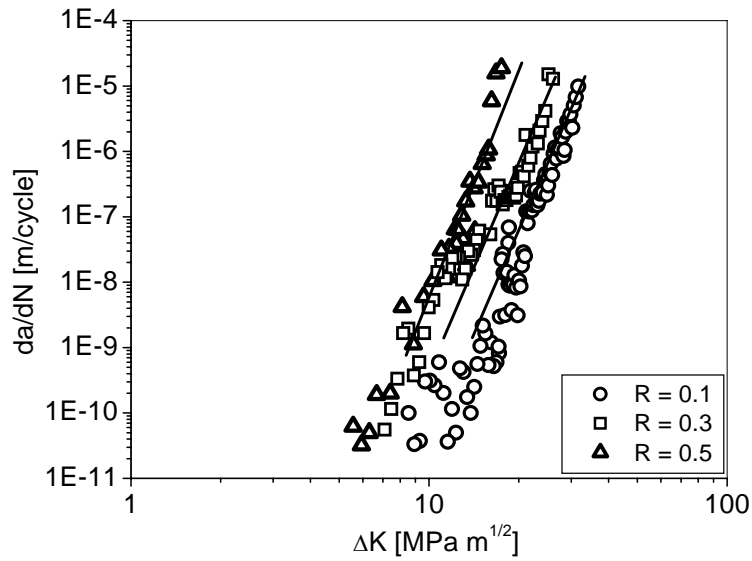


Fig. 2. Fatigue crack propagation ( $da/dN$ - $\Delta K$ ) curves for  $R = 0.1, 0.3$  and  $0.5$ .

Constant load tests at different load ranges of  $\Delta F = 4.6$  kN,  $\Delta F = 5.7$  kN and  $\Delta F = 6.8$  kN, corresponding to the initial stress intensity ranges of  $\Delta K = 16$   $\text{MPa m}^{0.5}$ ,  $\Delta K = 19$   $\text{MPa m}^{0.5}$  and  $\Delta K = 23$   $\text{MPa m}^{0.5}$ , respectively, were performed in order to clarify the crack growth behaviour in brazed components. Fig. 3 shows the crack length as a function of the number of loading cycles. It can be clearly seen that a slight increase of the applied load causes a significant increase of the crack growth rate.

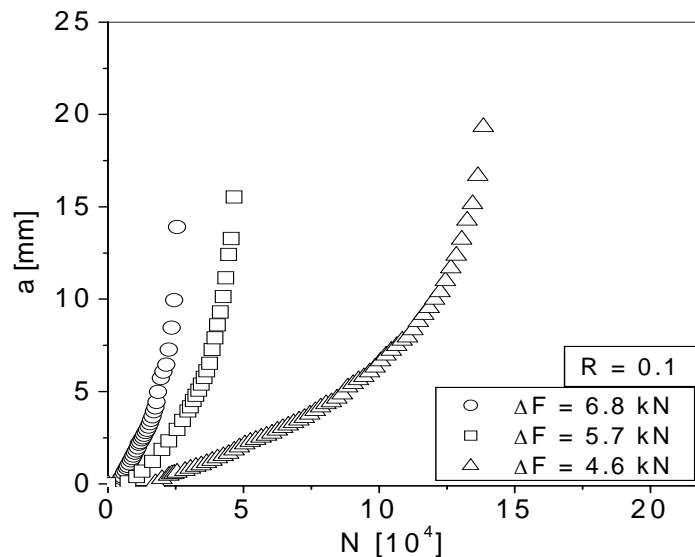


Fig. 3. Fatigue crack growth over number of loading cycles in constant tests at  $R = 0.1$ .

Table 3. Threshold values  $\Delta K_{th}$  and calculated C and n parameters at different R values.

R	$\Delta K_{th}$ (MPa m <sup>1/2</sup> )	C	n
0.1	9	1.309E-22	11.17
0.3	7	4.071E-23	12.17
0.5	6	7.234E-22	12.64

### 3.2. Microstructural and fractographic investigation

In order to characterize the fatigue crack propagation behaviour more precisely, the cross section of the DCB specimen was investigated by SEM after the test was stopped and the specimen was removed from the machine. Figure 4a shows the crack path beginning from the notch. The fine two phase microstructure of the AuNi18 filler metal, consisting of a Au rich solid solution (bright) and a Ni rich solid solution (grey) can be clearly seen. The crack initiated in the filler metal close to the steel/filler metal interface. Subsequently, it propagated along the centre line of the filler metal layer. In the following, several changes of the crack propagation path were observed. In Fig. 4b, jumps from one interface to the opposite one as well as from the interface to the filler metal center line can be seen.

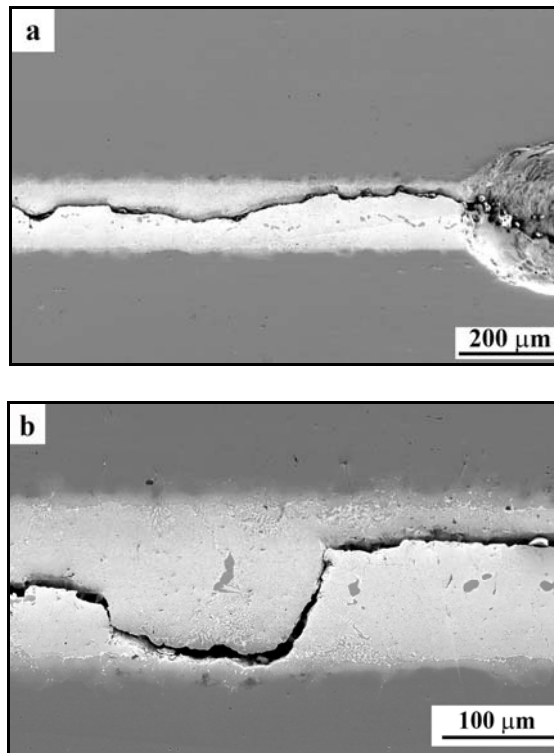


Fig. 4. SEM images of the cross section of the DCB specimen.

The fracture surfaces are depicted in Fig. 5. The macroscopic fatigue fracture patterns of the specimen were characterized by stereo microscopy (Fig. 5a). In contrast to bulk materials, no smooth fatigue fracture area could be observed. Instead, a stepped fracture pattern could be seen, which is in accordance to the observed crack path in Fig 4b.

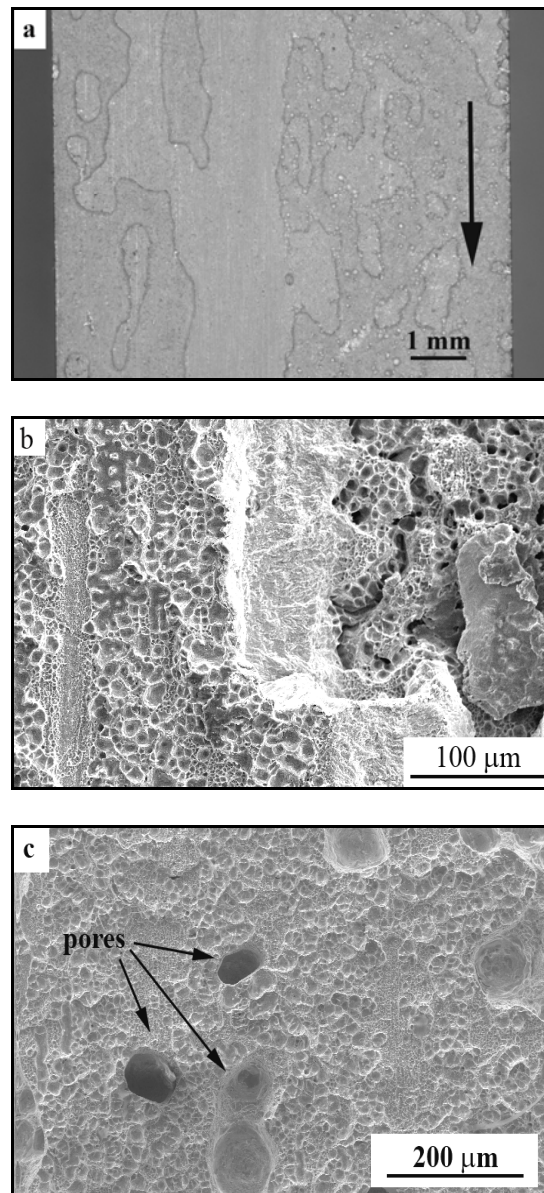


Fig. 5. Stereo microscope (a) and SEM images (b, c) of fracture surfaces. The arrow indicates the direction of crack propagation.

SEM investigations revealed ductile deformation features containing ductile dimples (Fig. 5b) on the fracture surface. Also at a higher magnification, the

stepped nature of the fracture pattern is clearly evident. Some pores that formed during the brazing process were also observed on the fracture surface (Fig. 5c).

#### 4. Discussion

In general the Paris exponent  $n$  is between 3 and 4 for most metals in the mid-growth rate regime. The  $n$  values for brazed martensitic stainless steel components as determined in this work are approximately 3 times higher (Table 3). Such high values are known only from brittle materials like ceramics, for which  $n$  values as high as 50 and above are reported [7, 14]. However, the fatigue damage mechanism is quite different from the one of ceramics. In fact, fractographic investigation showed plastic deformation features on the fracture surface (Fig. 5b) indicating ductile material damage during cyclic loading similar to the one in bulk metals. On the other hand, the measured threshold values,  $\Delta K_{th}$ , of brazed steel joints are significantly higher than those of bulk metallic materials. This indicates the presence of special shielding mechanisms in the vicinity of a crack in a thin plastic layer embedded in elastic material, including crack closure [19].

Phenomenologically, the high slope of the  $da/dN$ -curve which corresponds to the high  $n$ -values results from the relatively narrow band that is left between the relatively high threshold on the left hand side and the relatively low maximum  $\Delta K$ -value that can be reached under cyclic loading on the right hand side. The latter as well as the generally relatively high crack growth rates in the intermediate range are probably related to the complex triaxial stress state in the brazing zone, which is a result of the different elastic-plastic properties of the filler metal and the base material. The cyclic axial loading of brazed components leads to a periodically changing triaxial stress field in the filler metal layer, i.e to a state of multiaxial fatigue. As a result, a fatigue crack is not only subjected to mode I loading, but pronounced stresses parallel to the crack can occur, which increase the von-Mises-stress significantly, leading to increased stress and strain intensities at the crack tip and hereby to increased crack propagation rates [15]. Furthermore, it is known that in thin constrained metal layers under mode I loading high stresses of about four to six times the yield of the metal develop at a distance of several foil thicknesses ahead of the crack tip. These high stresses can lead to the formation of nanometer sized cavities at adjacent triggering sites (e.g second phase particles or interface pores) well ahead of the crack tip [16, 17, 18]. These cavities grow with increasing load and coalesce with each other, hereby forming larger cavities, before coalescence takes place near the main crack tip. These mechanisms have only been observed and described for constrained metal films subjected to static loading, but the damage and fracture behaviour of brazed joints under cyclic loading can be expected to behave similarly. After crack initiation, new cavities develop and grow ahead of the crack tip at microstructural inhomogeneities such

as large second phase particles which concentrate along the center line of the filler metal or close to the steel-AuNi18 interface during every loading cycle. The fatigue crack then propagates along these predamaged zones and coalesces with the cavities. This leads to a more pronounced increase of the crack length during every loading cycle as it would be the case in an undamaged material. It is possible that these mechanisms are very sensitive towards the stress intensity range, which would be a further explanation for the high  $n$  values. However, further investigations are required in the future.

## 5. Conclusions

In this present work, the fracture behaviour of HT brazed specimens of the martensitic stainless steel X3CrNiMo13-4 was investigated under cyclic loading. The influence of the load ratio  $R$  on the fatigue crack growth rates was underlined where crack growth rates are accelerated and  $\Delta K_{th}$  decreased with increasing  $R$  values. According to the steep slopes of the  $da/dN$ - $\Delta K$  curves, the obtained Paris exponent,  $n$ , was very high compared to homogenous materials. This observation was explained by the triaxial stress state in the filler metal, which is a result of the different elastic-plastic material properties of the filler metal and the base material.

## Acknowledgements

The present work was financially supported by MAN Turbo AG, Zürich. The authors would like to thank Dr. H. Gut.

## References:

- [1] S. L. Feldbauer, Modern Brazing of Stainless Steel, Weld. J. October 2004, 30.
- [2] J. Nowacki, P. Swider, Producibility of Brazed High-dimension Centrifugal Compressor Impellers, J. Mater. Proc. Tech. Vol. 133 (2003) 174.
- [3] C. Leinenbach, H. J. Schindler, T. A. Başer, N. Rüttimann, K. Wegener, Fracture Behaviour and Defect Assesment of Brazed Steel Joints, Proceedings of the 17<sup>th</sup> European Conference on Fracture-ECF17 (2008) 2121.
- [4] H. D. Solomon, A Statistical Analysis of Brazed Joint Fatigue Behaviour, Weld. Res. Suppl. 6 (2001) 148.
- [5] M. E. Kassner, T.C. Kennedy, K.K. Schrems, The Mechanism of Ductile Fracture in Constrained Thin Silver Films, Acta Mater. 46 (1998) 6445.

- [6] A. Tesch, R. Pippan, H. Döker, New Testing Procedure to Determine  $da/\Delta N$  Curves at Different Constant R-values Using One Single Specimen, *Int. J. Fatigue*, 29 (2007) 1220.
- [7] R. H. Dauskardt, A Frictional Wear Mechanism for Fatigue Crack Growth in Grain Bridging Ceramics, *Acta Metall. Mater.* 41 (1993) 2765.
- [8] J. Kohout, About the Dependence Between Exponent and Constant in the Paris Law for Fatigue Crack Growth Rate, *Proceedings of the 17<sup>th</sup> European Conference on Fracture-ECF17* (2008) 1083.
- [9] N. Singh, R. Khelawan, G. Marthur, Effect of Stress Ratio and Frequency on Fatigue Crack Growth Rate of 2618 Aluminium Alloy Silicon Carbide Metal Matrix Composite, *Bull. Mater. Sci.* 24 (2001) 169.
- [10] C. S. Kusko, J. N. Dupont, A. R. Marder, Influence of Stress Ratio on Fatigue Crack Propagation Behaviour of Stainless Steel Welds, *Weld. Res.* 2 (2004) 59.
- [11] S. C. Forth, J. C. Newman, R. G. Forman, On Generating Fatigue Crack Growth Thresholds, *Int. J. Fatigue* 25 (2003) 9.
- [12] H. Döker, Fatigue Crack Growth Treshold: Implications, Determination and Data Evaluation, *Int. J. Fatigue* 19 (1997) 145.
- [13] ASTM E647, Standart Test Method for Measurement of Fatigue Crack Growth Rates, *Annual book of ASTM standards, Section 3 vol. 03.01* (2001).
- [14] S. Li, L. Sun, W. Jia, Z. Wang, The Paris Law in Metals and Ceramics, *J. Mater. Sci Lett.* 14 (1995) 1493.
- [15] D. Tchankov, M. Sakane, T. Itoh, N. Hamada, Crack opening displacement approach to assess multiaxial low cycle fatigue, *Int. J. Fatigue* 30 (2008) 417.
- [16] M. C. Tolle, M. E. Kassner, E. Cerri, R. S. Rosen, Mechanical Behaviour and Microstructure of Au-Ni Brazes, *Metall. Mater. Trans.* 26 (1995) 941.
- [17] A. G. Varias, Z. Suo, C. F. Shih, Ductile Failure of a Constrained Metal Foil, *J. Mech. Phys. Solids* 39 (1991) 963.
- [18] S. R. Chowdhury, R. Narasimhan, Ductile Failure in a Constrained Metal Layer Under Mixed Mode Loading, *Acta Mater.* 46 (1998) 1103.
- [19] H. J. Schindler, On the Significance of Crack Tip Shielding in Fatigue Threshold - Theoretical Relations and Experimental Implications, *Fatigue Crack Growth Thresholds, Endurance Limits, and Design, ASTM STP 1372*, J. C. Newman and R. S. Piascik, Eds., American Society for Testing and Materials, West Conshohocken, PA (1999).